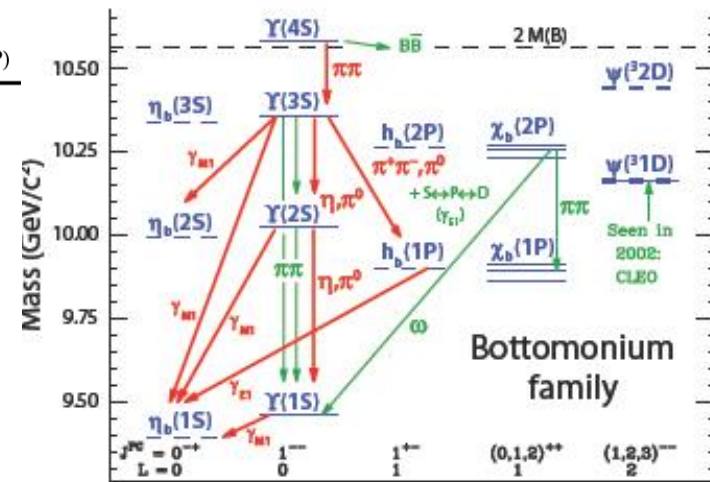
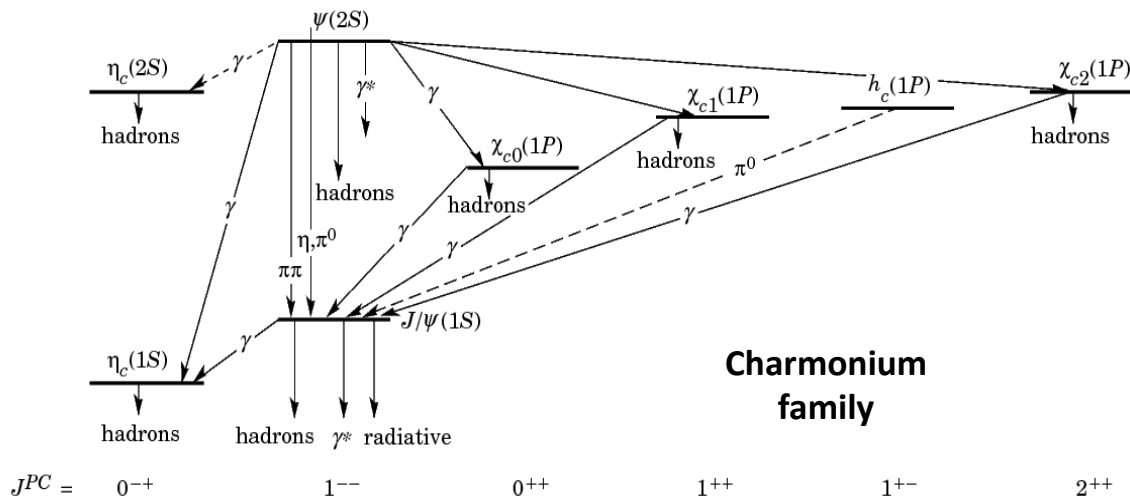


Measurement of Quarkonium Production with CMS in pp Collisions at $\sqrt{s} = 7$ TeV

Andrew York (University of Tennessee),
on behalf of the CMS Collaboration



Overview

- Motivations to study quarkonium production
- Overview of CMS detector and analysis techniques
- Production rates:
 - J/ψ and $\psi(2S)$ production
 - $Y(nS) \rightarrow \mu^+\mu^-$ production
 - Relative prompt production of χ_{c1} and χ_{c2}
- First observed decays in CMS:
 - Observation of $B_c^\pm \rightarrow J/\psi \pi^\pm$ and $B_c^\pm \rightarrow J/\psi \pi^\pm \pi^\pm \pi^\mp$
- Summary

Motivations to Study Quarkonium Production

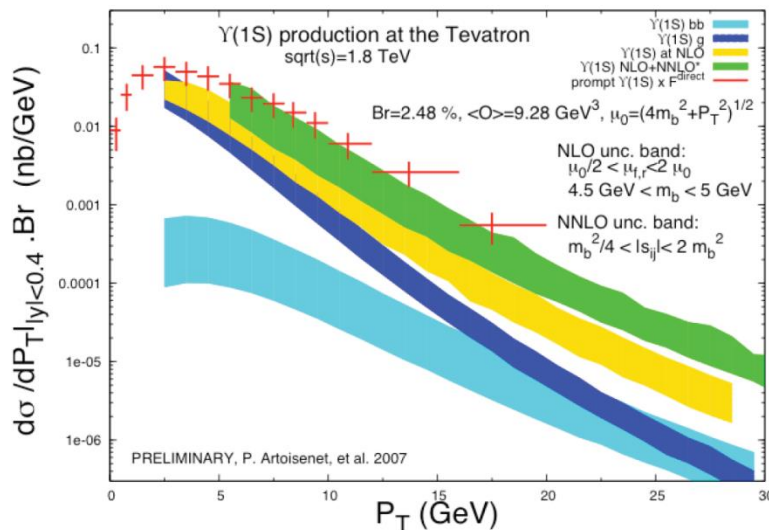
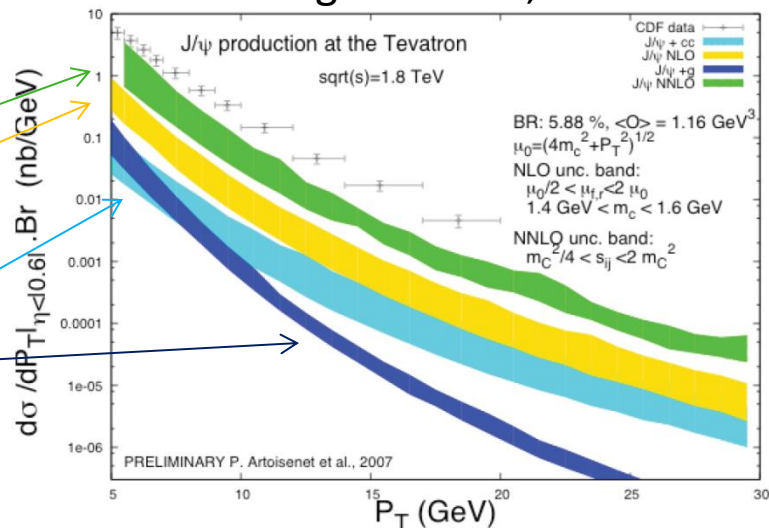
Motivation: no theory has simultaneously explained measured production cross-sections and polarizations

New experimental reach:

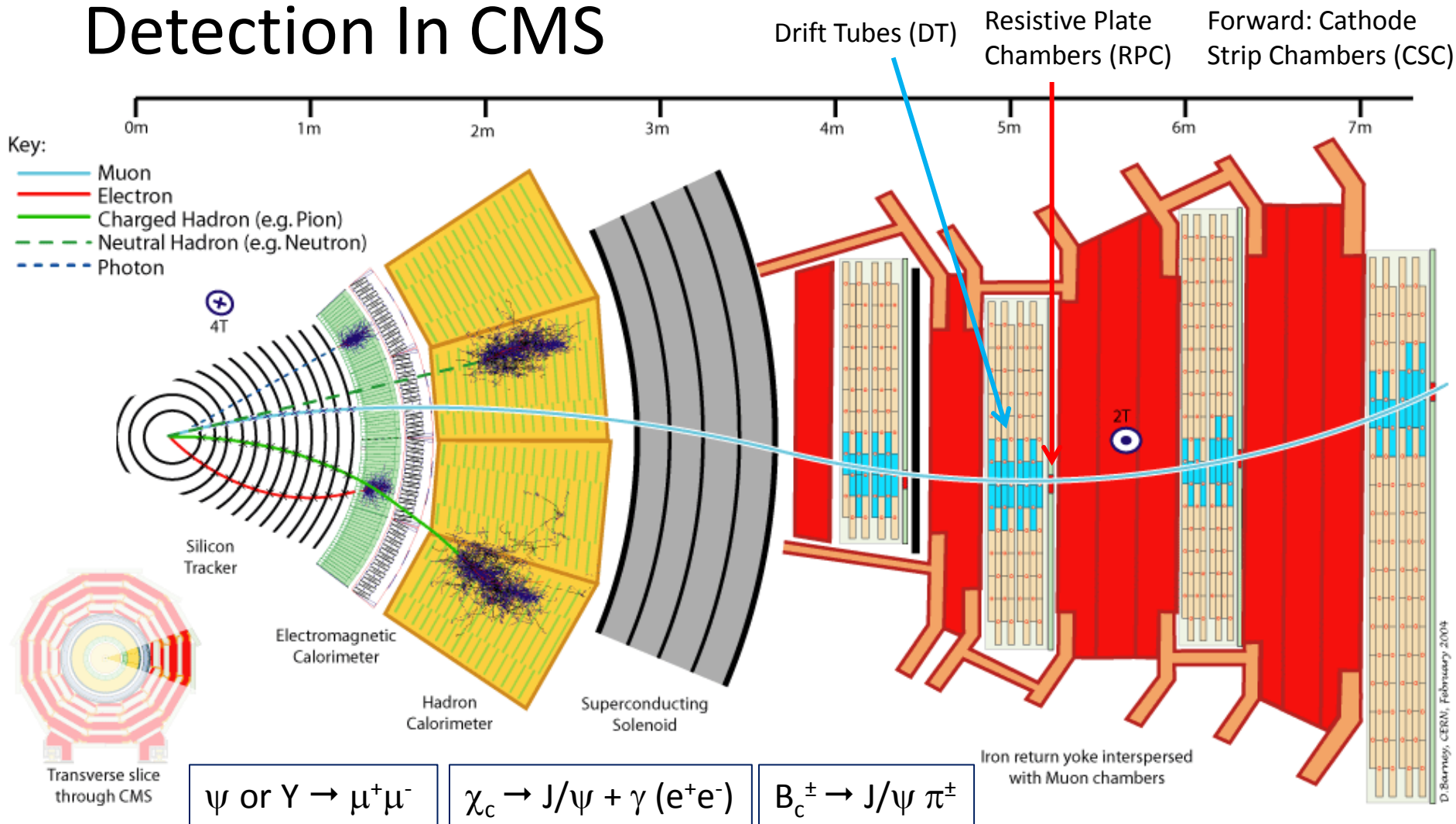
- LHC extends the frontier for collisions
 - Increased energy and luminosity
 - gg fusion dominates production
- CMS provides:
 - Excellent dimuon mass resolution
 - Excellent photon resolution through $\gamma \rightarrow e^+e^-$ conversion

NNLO
NLO
LO associate
LO direct

Color Singlet Model, Tevatron



Detection In CMS

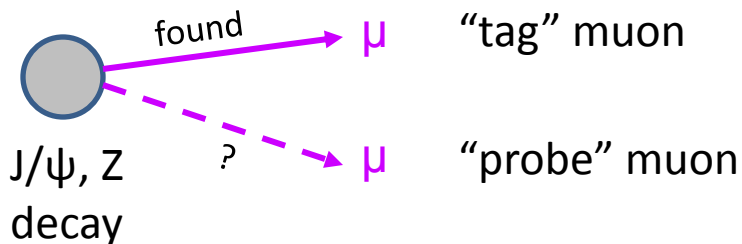


- **Track building:** charge deposits in silicon pixel/strip tracker propagated from Pixel hit trajectories, $\sigma_{pT}/pT \sim 1\%$
- **Muon building:** charge deposits in DT/RPC layer merged into hits, propagated to beamspot to form segments. Tracks matched to muon segments.

Muon Efficiency in CMS

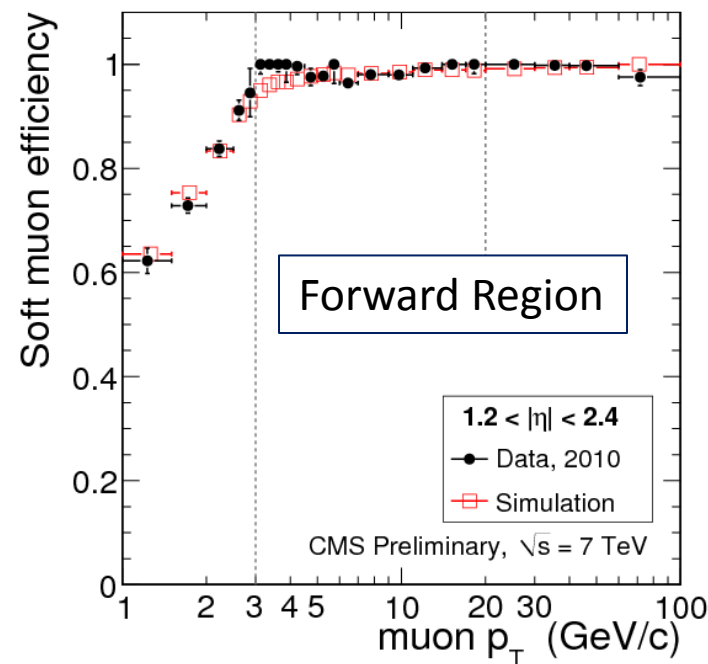
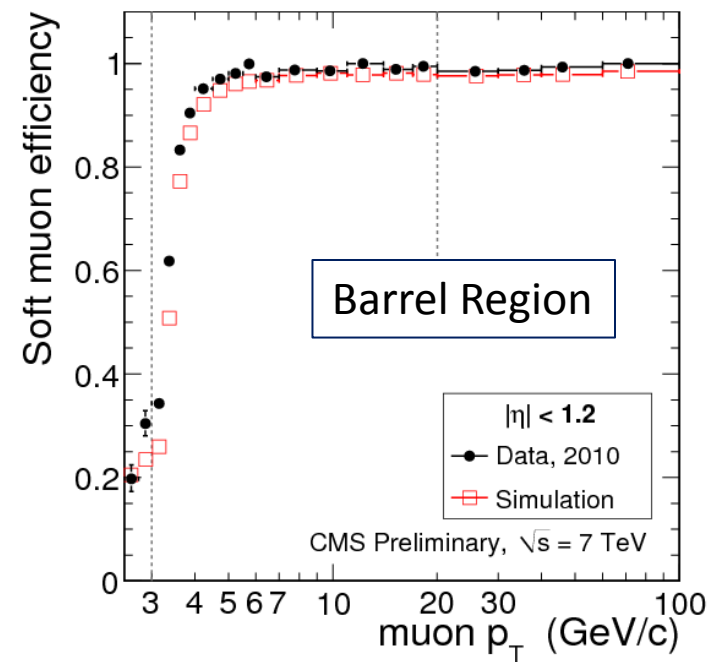
$$\epsilon_{\mu} = \epsilon_{\text{trig}} * \epsilon_{\text{track}} * \epsilon_{\text{MuonID}}$$

Muon efficiency measured in data using “tag and probe” technique



(simulation compatible with data)

Efficient over wide range of momentum and angular coverage



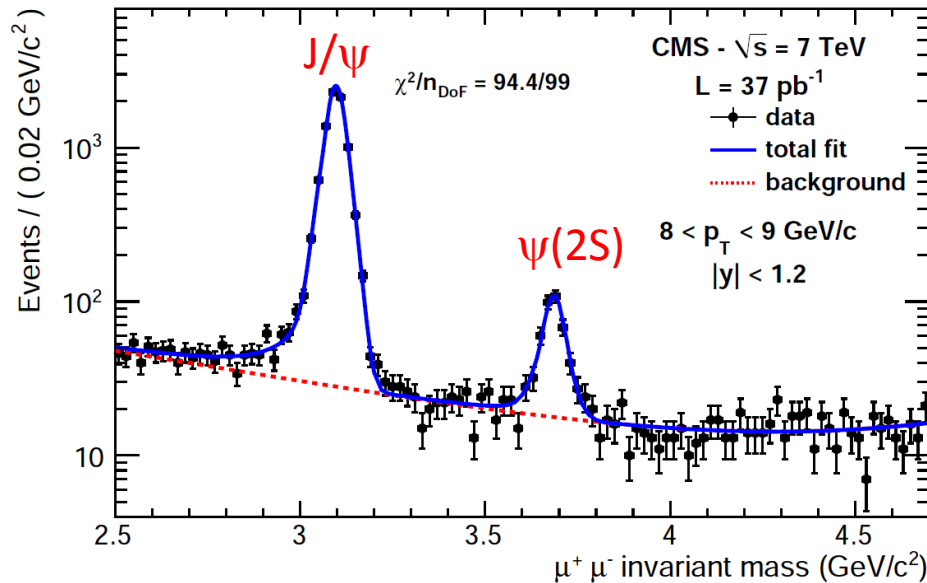
Signal Extraction

Discriminating variable: $\mu^+\mu^-$ Invariant Mass

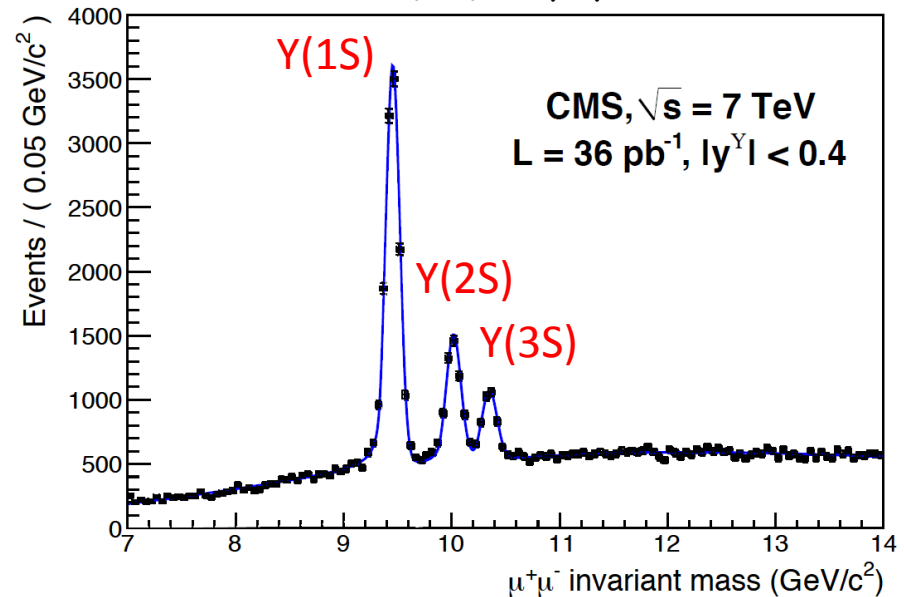
Parameterization: Crystal Ball and/or Gaussian for signal, exponential or product of exponential and error function for background

Maximum Likelihood fit: with mass differences fixed to PDG values, common resolution value scaled by mass

$\psi(nS) \rightarrow \mu^+\mu^-$



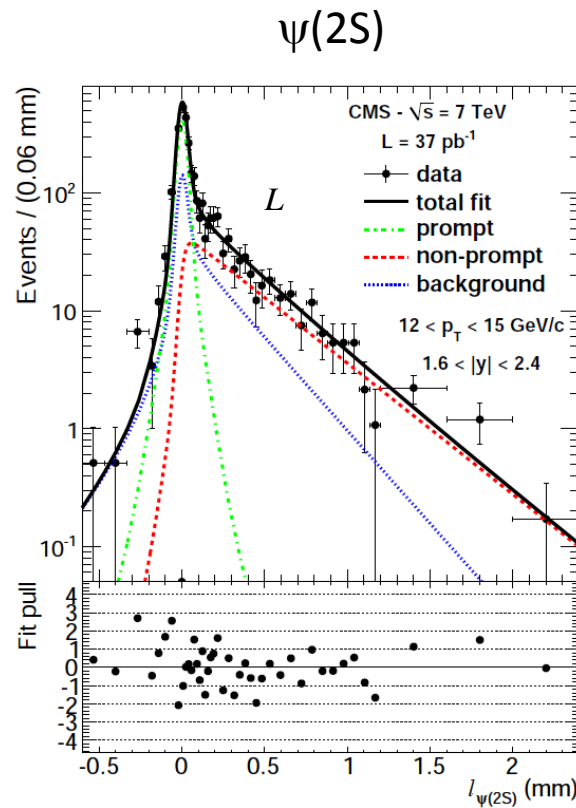
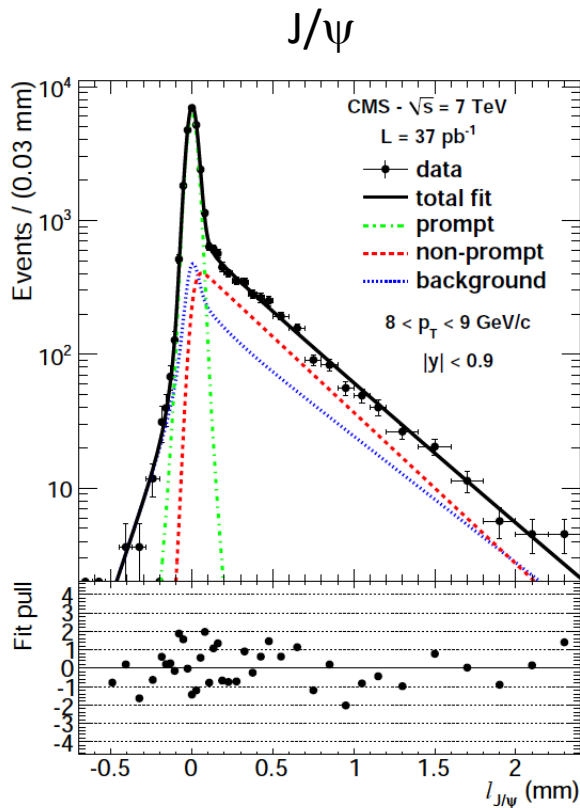
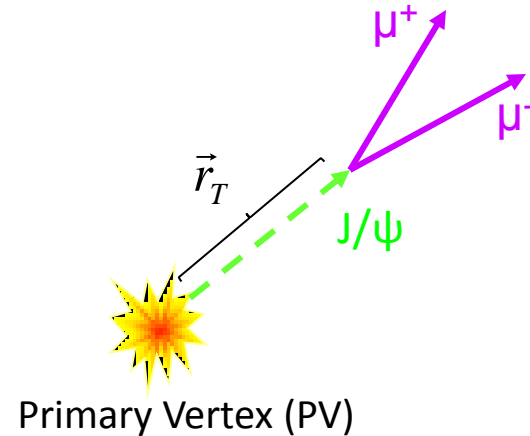
$Y(nS) \rightarrow \mu^+\mu^-$



Separating Prompt and Non-prompt J/ψ

ML Fit as before, with addition of pseudo-proper decay length variable (l_{xy})

Parameterization: double Gaussian for resolution, times exponential decay for non-prompt



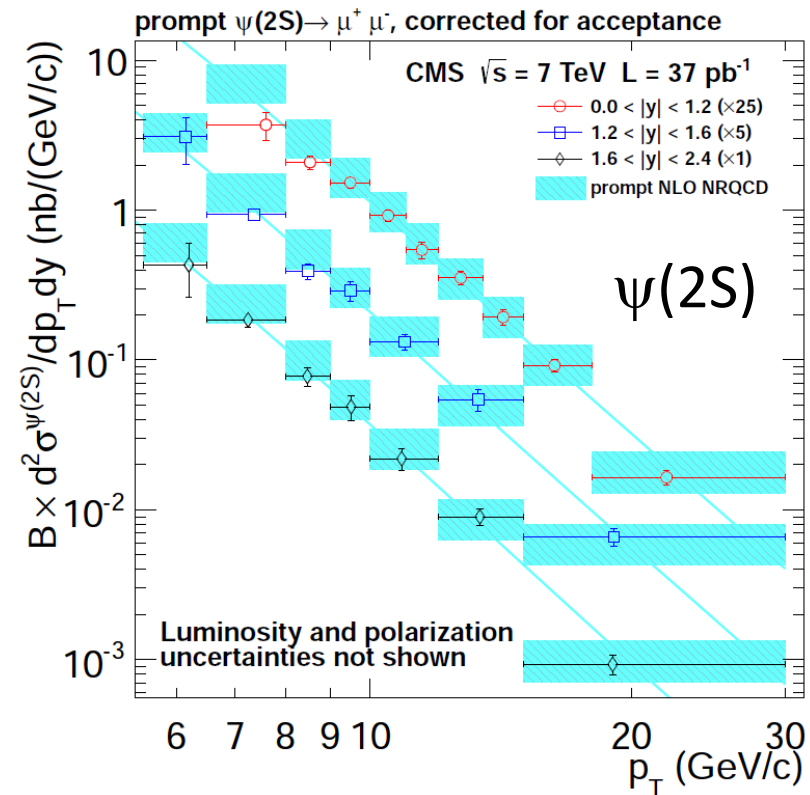
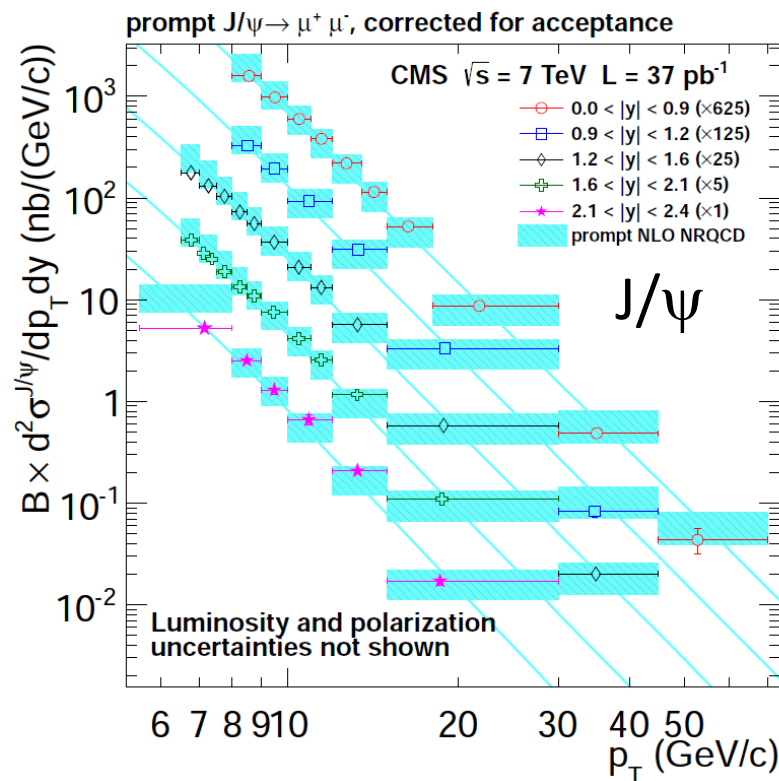
$$L_{xy}^{J/\psi} = \frac{\vec{r}_T \cdot \vec{p}_T^{J/\psi}}{|\vec{p}_T^{J/\psi}|}$$

$$l_{xy} = \frac{M^{J/\psi}}{|\vec{p}_T^{J/\psi}|} L_{xy}^{J/\psi}$$

J/ψ and ψ(2S) Production

JHEP 02 (2012), 011

Prompt cross-section results:



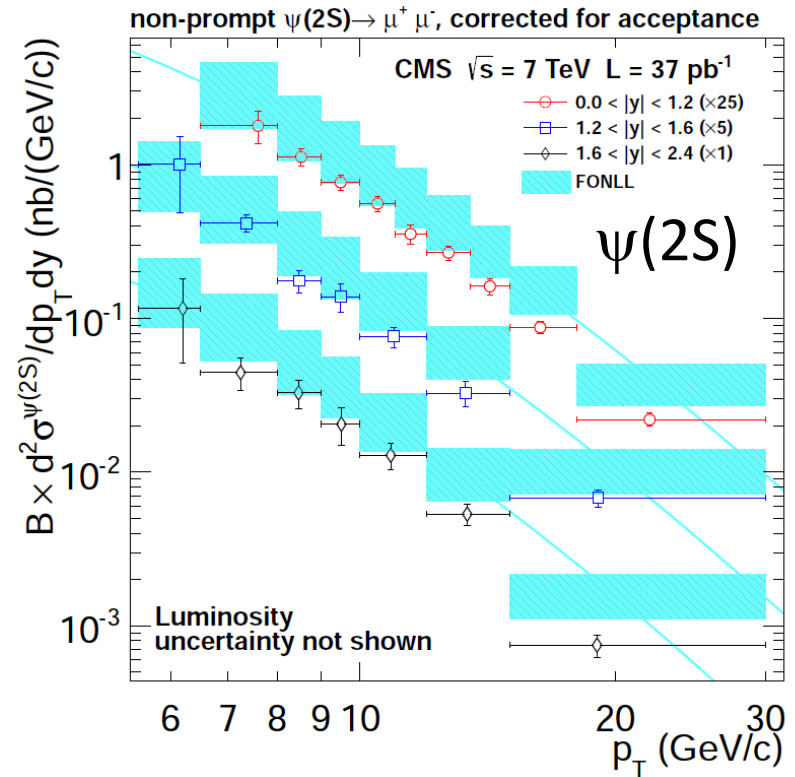
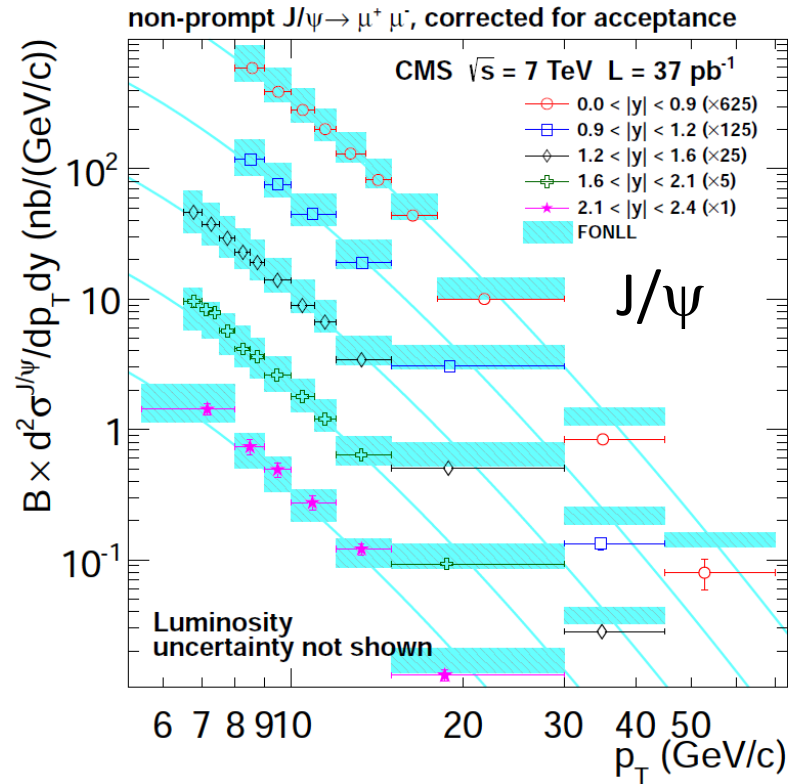
Agrees with NRQCD predictions

- Theory based on CS+CO model at NLO
- Feed-down effect included in theory

J/ψ and ψ(2S) Production

JHEP 02 (2012), 011

Non-prompt cross-section results:



Predictions based on Fixed Order plus Next to Leading Logs (FONLL)
- Fall at high p_T compared to theory, overall shift in ψ(2S) case

J/ψ and ψ(2S) Production

JHEP 02 (2012), 011

Improved branching fraction determination using

- from PDG: $\mathcal{B}(B \rightarrow J/\psi X)$, $\mathcal{B}(\psi(2S) \rightarrow \mu^+\mu^-)$, $\mathcal{B}(J/\psi \rightarrow \mu^+\mu^-)$
- from measurement:

$$R(p_T, |y|) = \frac{\frac{d^2\sigma}{dp_T dy}(\psi(2S)) \cdot \mathcal{B}(\psi(2S) \rightarrow \mu^+\mu^-)}{\frac{d^2\sigma}{dp_T dy}(J/\psi) \cdot \mathcal{B}(J/\psi \rightarrow \mu^+\mu^-)} = \frac{N_{\psi(2S)}^{\text{corr}}(p_T, |y|)}{N_{J/\psi}^{\text{corr}}(p_T, |y|)}$$

Determination made as:

$$\mathcal{B}(B \rightarrow \psi(2S)X) = \frac{R \cdot \sigma(J/\psi) \cdot \mathcal{B}(B \rightarrow J/\psi X) \cdot \mathcal{B}(J/\psi \rightarrow \mu^+\mu^-)}{\sigma(\psi(2S)) \cdot \mathcal{B}(\psi(2S) \rightarrow \mu^+\mu^-)}$$

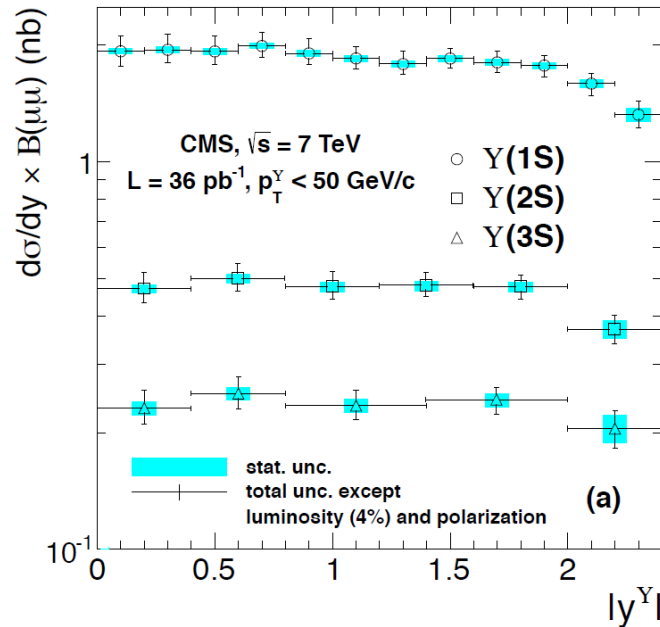
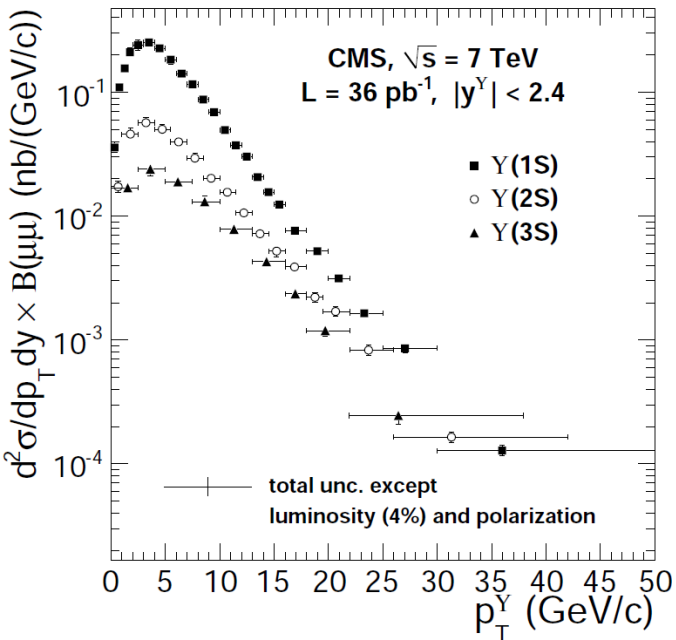
with result:

$$\mathcal{B}(B \rightarrow \psi(2S)X) = (3.08 \pm 0.12 \text{ (stat.+syst.)} \pm 0.13 \text{ (theor.)} \pm 0.42 \text{ (}\mathcal{B}_{\text{PDG}}\text{)}) \times 10^{-3}$$

$\Upsilon(nS) \rightarrow \mu^+\mu^-$ Production

arXiv:1303.5900

Production cross-section results:



$\Upsilon(nS)$ acceptance regime:

- $p_T < 50 \text{ GeV}/c$
- $|y| < 2.4$

assumes unpolarized production

$$\sigma(pp \rightarrow \Upsilon(1S)X) \cdot \mathcal{B}(\Upsilon(1S) \rightarrow \mu^+\mu^-) = (8.55 \pm 0.05^{+0.56}_{-0.50} \pm 0.34) \text{ nb},$$

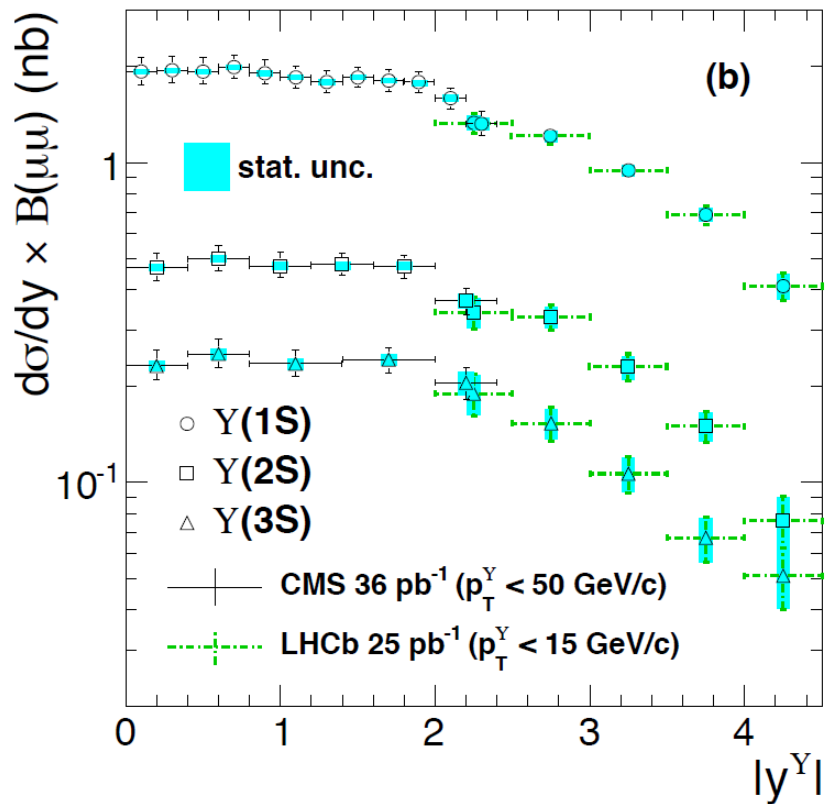
$$\sigma(pp \rightarrow \Upsilon(2S)X) \cdot \mathcal{B}(\Upsilon(2S) \rightarrow \mu^+\mu^-) = (2.21 \pm 0.03^{+0.16}_{-0.14} \pm 0.09) \text{ nb},$$

$$\sigma(pp \rightarrow \Upsilon(3S)X) \cdot \mathcal{B}(\Upsilon(3S) \rightarrow \mu^+\mu^-) = (1.11 \pm 0.02^{+0.10}_{-0.10} \pm 0.04) \text{ nb},$$

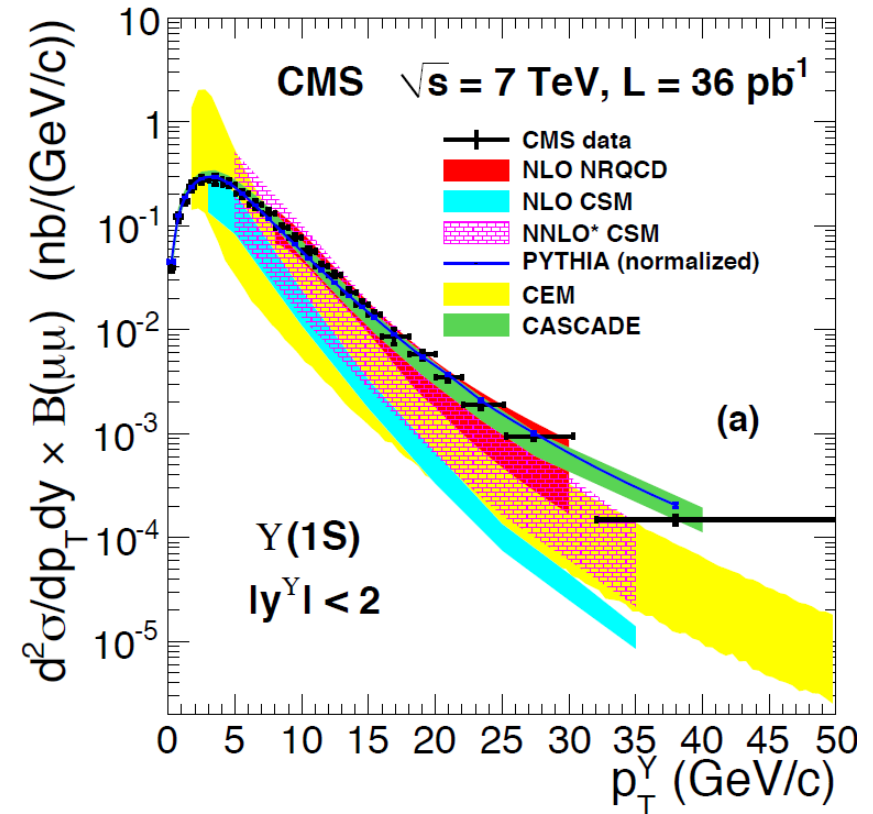
$Y(nS) \rightarrow \mu^+\mu^-$ Production

arXiv:1303.5900

Comparison to LHCb and theory:



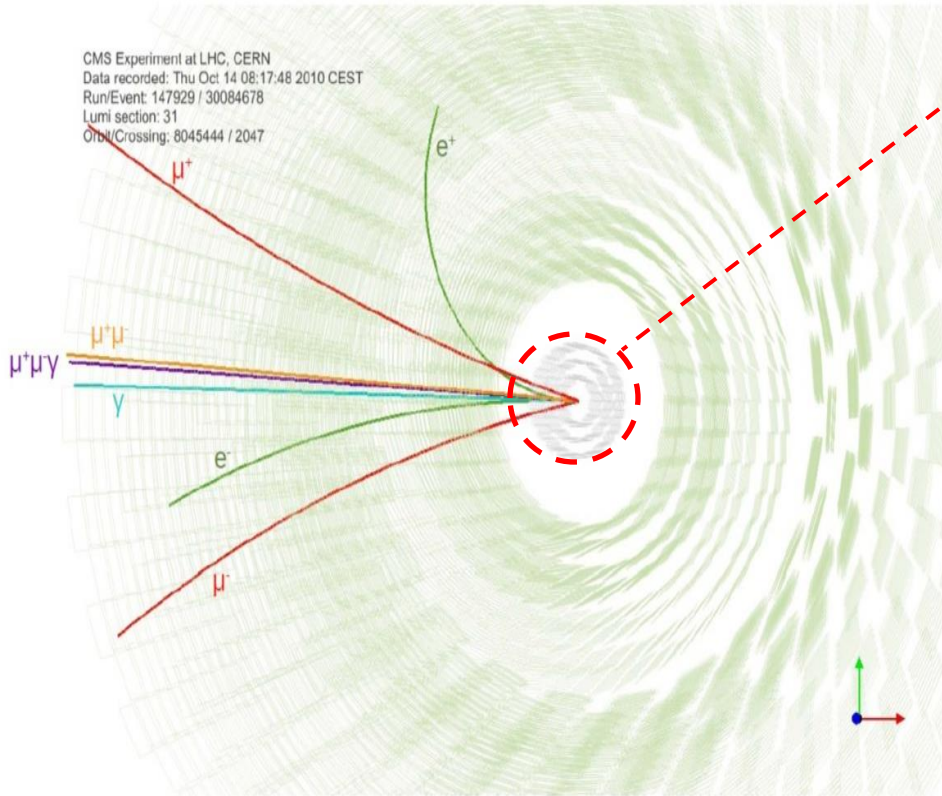
Complements LHCb and consistent in region of overlap



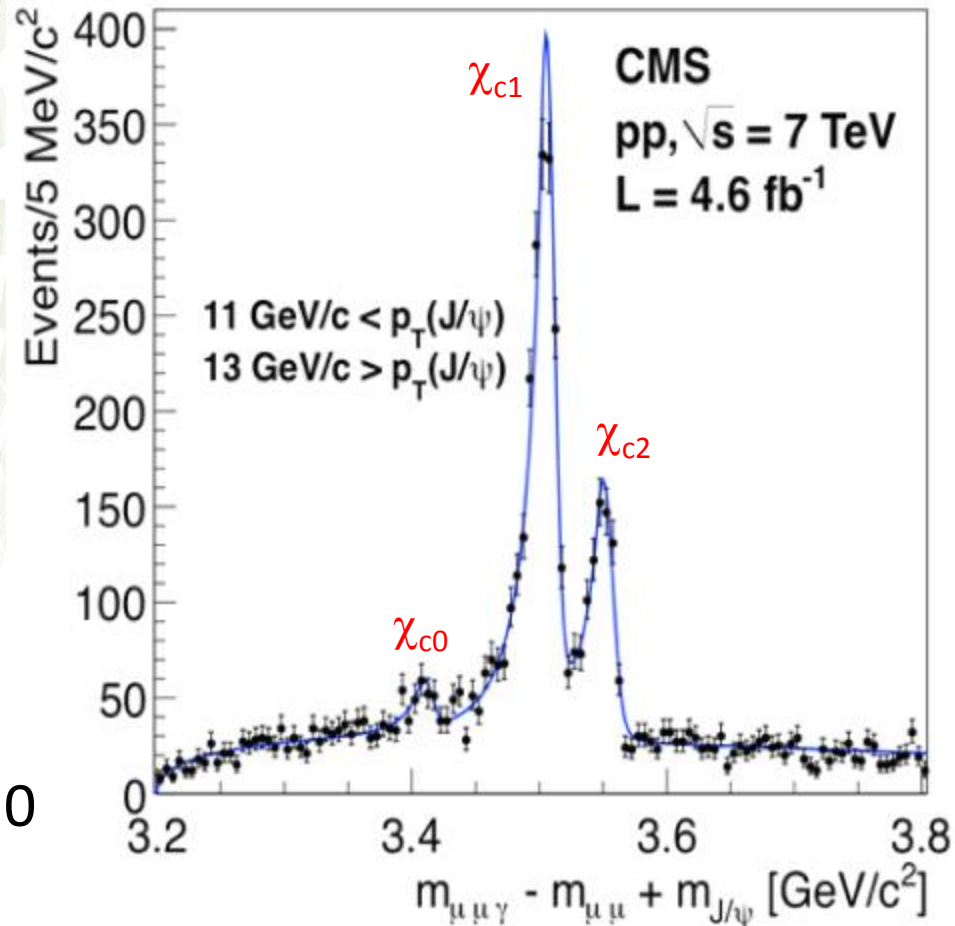
Best agreement with CASCADE and NRQCD (CS+CO at NLO)

Relative Prompt Production Rate of χ_{c1} and χ_{c2}

EPJC 72 (2012), 2251



most reconstructed photons converted in beampipe and Pixel layers

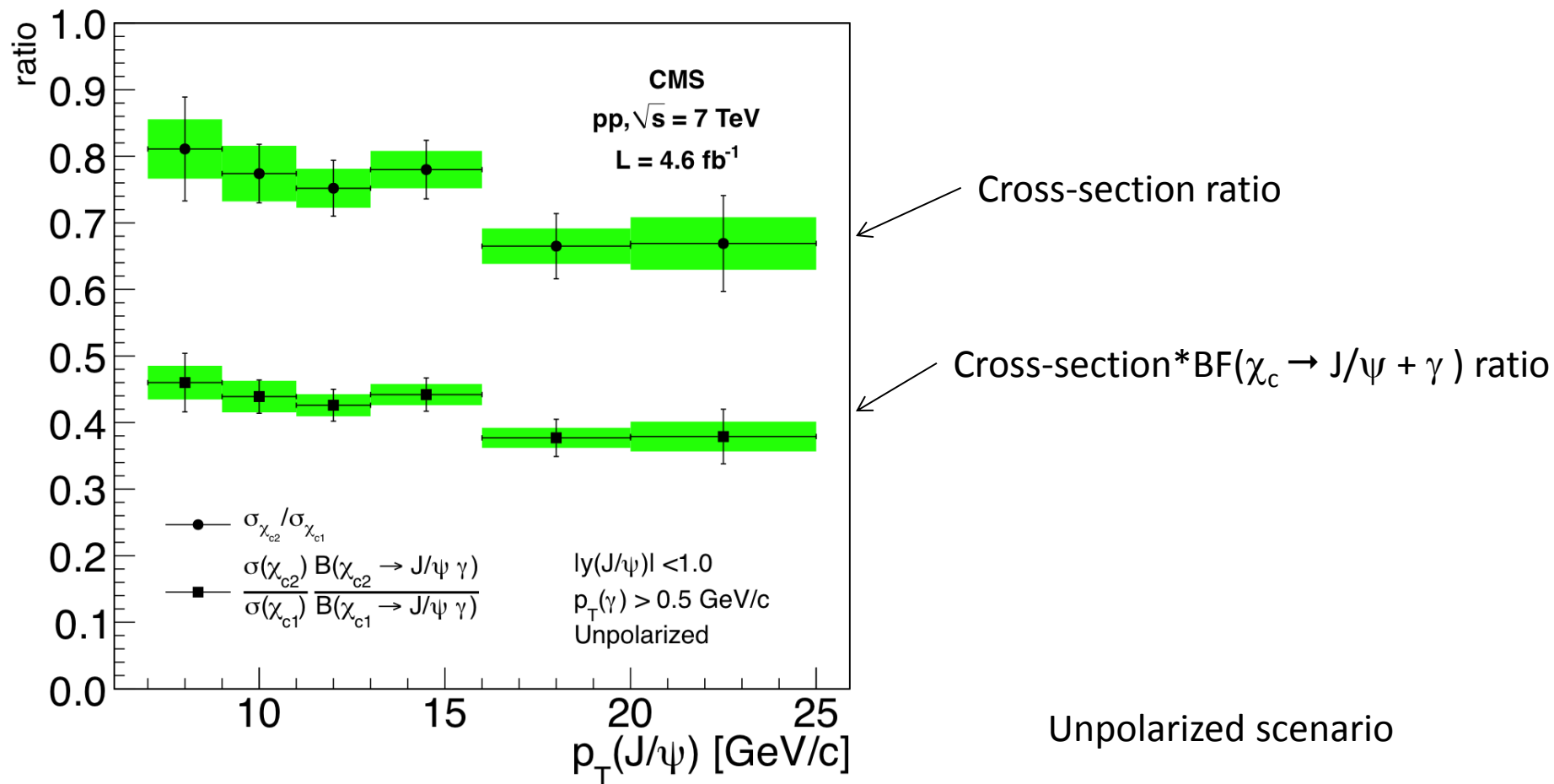


- Identified using radiative decay $\chi_c \rightarrow J/\psi + \gamma$ where $\gamma \rightarrow e^+e^-$
- With requirements: $|\gamma(J/\psi)| < 1.0$ and $p_T(\gamma) > 0.5 \text{ GeV}/c$

Relative Prompt Production Rate of χ_{c1} and χ_{c2}

EPJC 72 (2012), 2251

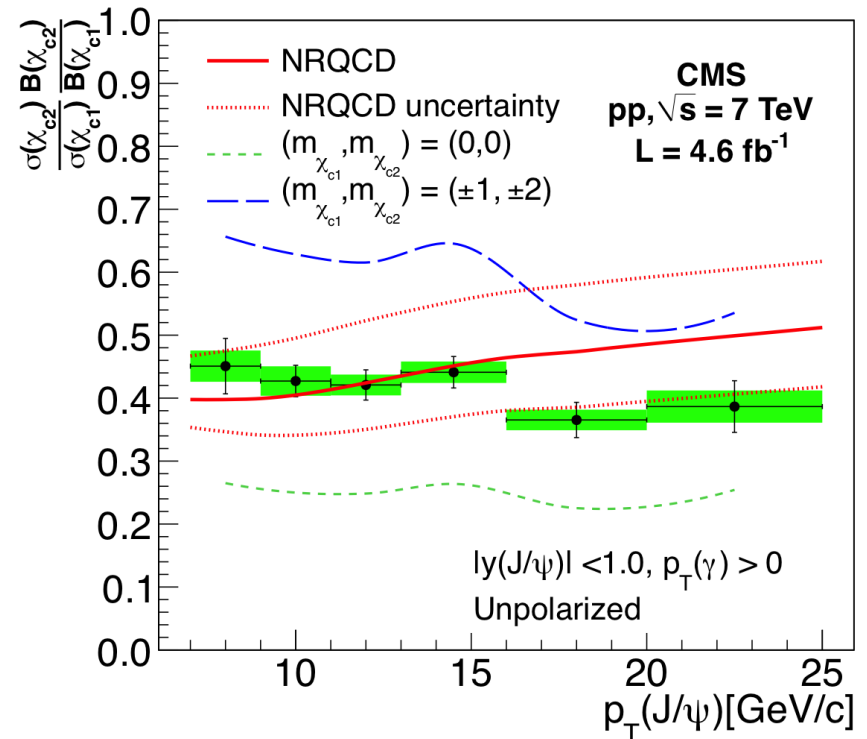
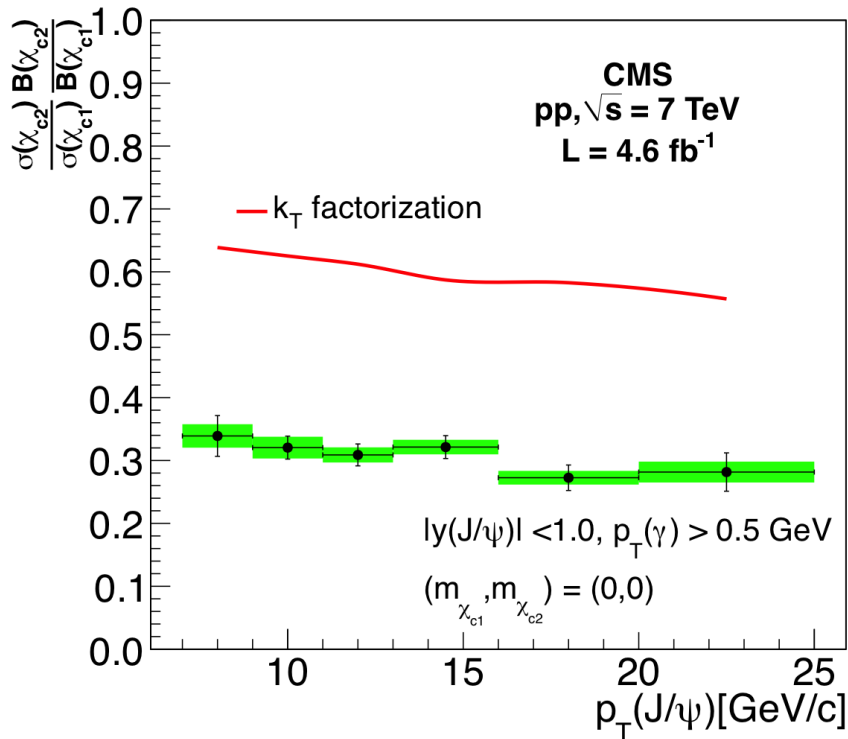
Results:



Relative Prompt Production Rate of χ_{c1} and χ_{c2}

EPJC 72 (2012), 2251

Comparison to theory:



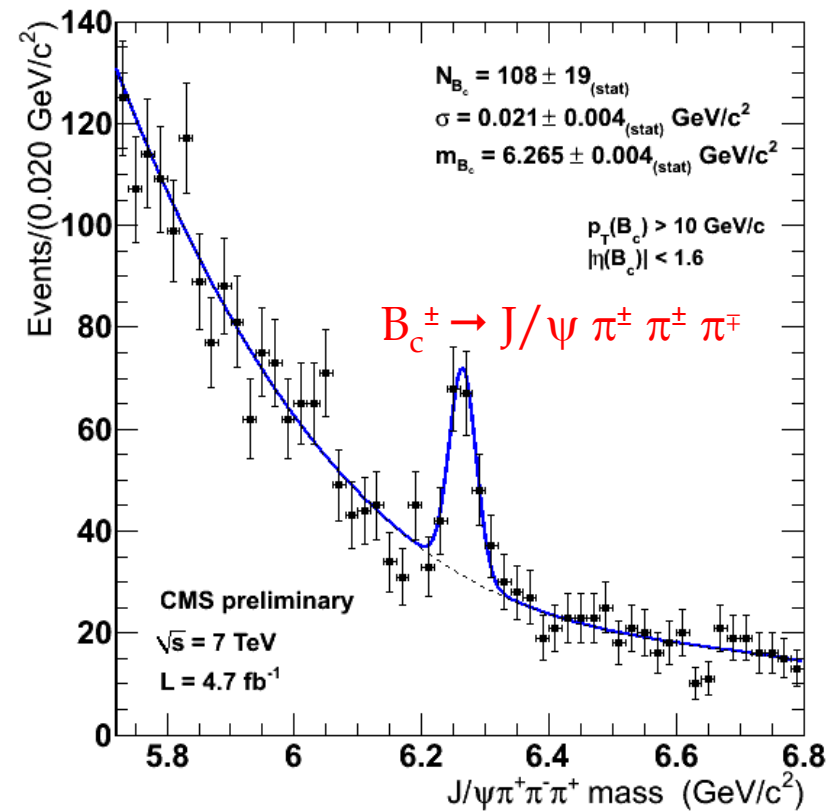
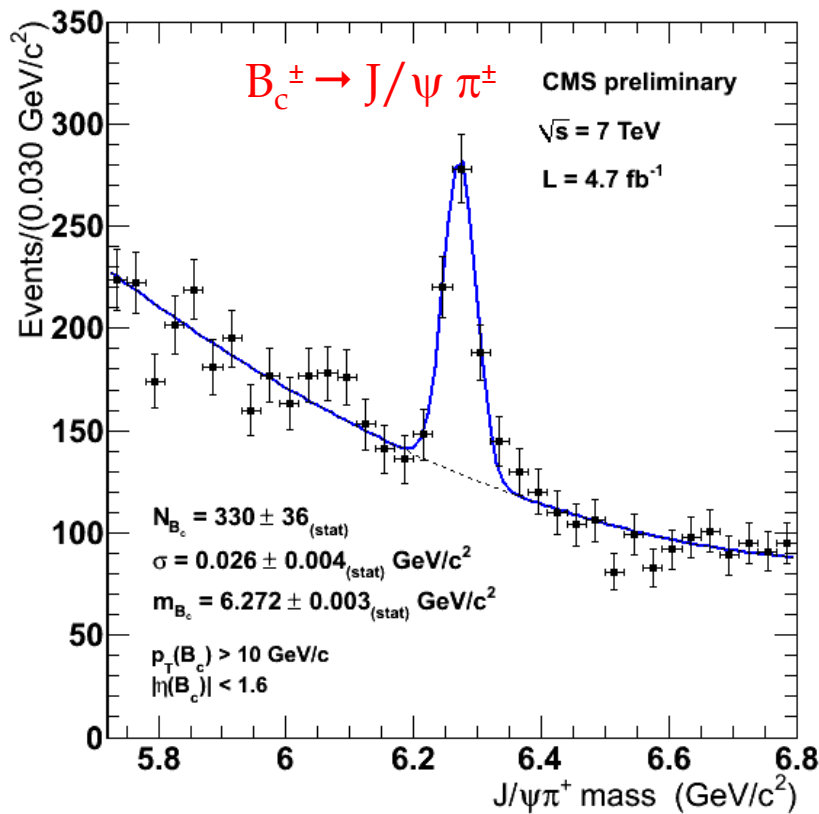
- k_T factorization describes shape, but not the level of χ_{c2}/χ_{c1} ratio
- NRQCD (CS+CO at NLO) provides agreement within uncertainty (data extrapolated back to $p_T(\gamma) > 0$ phase space for comparison)

Observation of $B_c^\pm \rightarrow J/\psi \pi^\pm$ and $B_c^\pm \rightarrow J/\psi \pi^\pm \pi^\pm \pi^\mp$

CMS-PAS-BPH-11-003

$$B_c^\pm \rightarrow J/\psi \pi^\pm : S/\sqrt{S+B} = 10.5$$

$$B_c^\pm \rightarrow J/\psi \pi^\pm \pi^\pm \pi^\mp : S/\sqrt{S+B} = 6.1$$



Summary

- J/ψ , $\psi(2S)$, and $Y(nS)$ differential cross-sections measured with uncertainties (statistical+systematic) of 20% or less
 - Complementary coverage to LHCb
 - Production rates agree with NRQCD predictions
 - Reduces relative uncertainty of $\mathcal{B}(B \rightarrow \psi(2S) X)$ agrees with world average value, improves relative uncertainty by factor of 3
- Production ratio χ_{c2}/χ_{c1} measured
 - Extends pT measurement beyond previous experiments
 - Most precise measurement to date!
- Observation of $B_c \rightarrow J/\psi \pi^\pm$ and $B_c \rightarrow J/\psi \pi^\pm \pi^\pm \pi^\mp$ decays provide first fully reconstructed observation of B_c decays in CMS (needed for lifetime measurement)

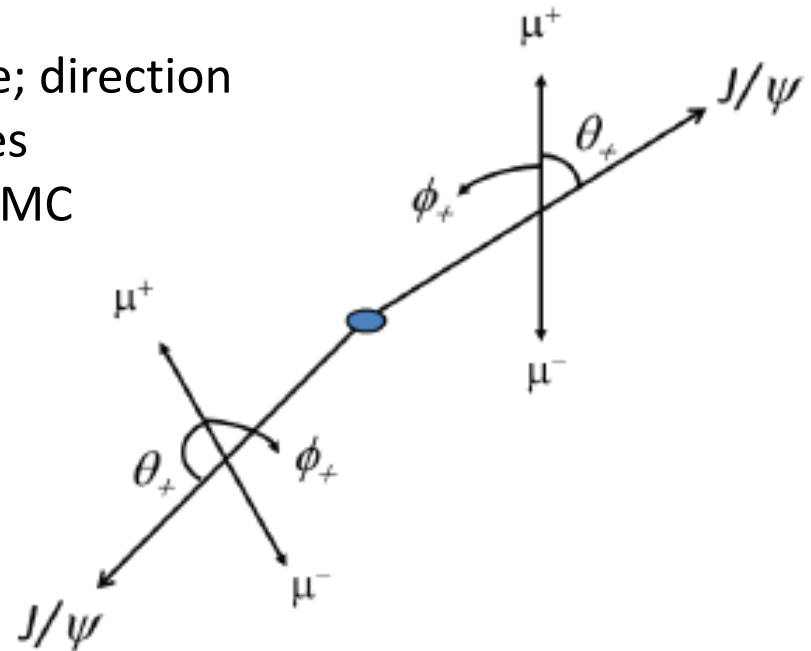
Backup

Acceptance and Polarization Uncertainty

Acceptance

Decay particles uniformly in their own rest frame; direction along flight path is reference axis for decay angles

- Determine acceptance value per bin based on MC



Uncertainty

Instead of assuming muons are produced uniformly in J/ψ rest frame, assume distribution of:

$$\frac{dN}{d \cos \theta_+} \propto 1 + \lambda_\theta \cos^2 \theta_+$$

→ Test acceptance limits by testing extremes of decay distribution, ie $\lambda_\theta = +1, -1$

Photon Conversion Radii

CMS coll., EPJC 72 (2012), 2251

